Science Translational Medicine
AAAS

stm.sciencemag.org/cgi/content/full/13/584/eaay9056/DC1

# Supplementary Materials for

## Long-lasting analgesia via targeted in situ repression of $Na_V1.7$ in mice

Ana M. Moreno, Fernando Alemán, Glaucilene F. Catroli, Matthew Hunt, Michael Hu, Amir Dailamy, Andrew Pla, Sarah A. Woller, Nathan Palmer, Udit Parekh, Daniella McDonald, Amanda J. Roberts, Vanessa Goodwill, Ian Dryden, Robert F. Hevner, Lauriane Delay, Gilson Gonçalves dos Santos, Tony L. Yaksh*, Prashant Mali*

*Corresponding author. Email: pmali@ucsd.edu (P.M.); tyaksh@ucsd.edu (T.L.Y.)

Published 10 March 2021, *Sci. Transl. Med.* **13**, eaay9056 (2021)
DOI: 10.1126/scitranslmed.aay9056

**This PDF file includes:**

## MATERIALS AND METHODS

*Vector Design and Construction*

dCas9 and Zinc-Finger AAV vectors were constructed by sequential assembly of corresponding gene blocks (Integrated DNA Technologies) into a custom synthesized rAAV2 vector backbone. gRNA sequences were inserted into dNCas9 plasmids by cloning oligonucleotides (IDT) encoding spacers into AgeI cloning sites via Gibson assembly. gRNAs were designed utilizing an in silico tool to predict gRNAs *(73)*. For in vivo KRAB-dCas9 experiments, a dual-gRNA design was used (guides SCN9A-1 and SCN9A-2), except for the paclitaxel-induced neuropathic pain model in **Fig. 5**, which only utilized a single-gRNA (gRNA 2). ZF computational designs were obtained via Sigma.

*Mammalian Cell Culture*

Neuro2a cells were grown in EMEM supplemented with 10% fetal bovine serum (FBS) and 1% Antibiotic-Antimycotic (Thermo Fisher Scientific) in an incubator at 37°C and 5% $CO_2$ atmosphere.

*Lipid-Mediated Cell Transfections*

One day prior to transfection, Neuro2a cells were seeded in a 24-well plate at a cell density of 1 or 2 × $10^5$ cells per well. 0.5 µg of each plasmid was added to 25 µL of Opti-MEM medium, followed by addition of 25 µL of Opti-MEM containing 2 µL of Lipofectamine 2000. The mixture was incubated at room temperature for 15 min. The entire solution was then added to the cells in a 24-well plate and mixed by gently swirling the plate. Media was changed after 24 h, and the plate was incubated at 37°C for 72 h in a 5% $CO_2$ incubator. Cells were harvested, spun down, and frozen at 80°C.

*Production of AAVs*

Virus was prepared by the Gene Transfer, Targeting and Therapeutics (GT3) core at the Salk Institute of Biological Studies (La Jolla, CA) or in-house utilizing the GT3 core protocol. Briefly, AAV2/9 virus particles were produced using HEK293T cells via the triple transfection method and purified via an iodixanol gradient. Confluency at transfection was between 80% and 90%. Media was replaced with pre-warmed media

2h before transfection. Each virus was produced in five 15 cm plates, where each plate was transfected with 10 µg of pXR-capsid (pXR-9), 10 of µg recombinant transfer vector, and 10 µg of pHelper vector using polyethylenimine (PEI; 1 mg/mL linear PEI in DPBS [pH 4.5], using HCl) at a PEI:DNA mass ratio of 4:1. The mixture was incubated for 10 min at room temperature and then applied dropwise onto the media. The virus was harvested after 72 h and purified using an iodixanol density gradient ultracentrifugation method. The virus was then dialyzed with 1x PBS (pH 7.2) supplemented with 50 mM NaCl and 0.0001% of Pluronic F68 (Thermo Fisher Scientific) using 50-kDa filters (Millipore) to a final volume of ~100 µL and quantified by qPCR using primers specific to the ITR region, against a standard (ATCC VR-1616): AAV-ITR-F: 5' -CGGCCTCAGTGAGCGA-3' and AAV-ITR-R: 5' -GGAACCCCTAGTGATGGAGTT-3'

*Whole-DRG mounts*

21 Days following i.t. injections of AAV9-mCherry, mice were transcardially perfused with 4% PFA and post-fixed in 4% PFA for 24 hours, then stored in PBS with 0.02% sodium azide. DRGs from cervical, thoracic, lumbar and sacral were dissected out and immediately cleared following the previously described RTF method *(74)*. In brief DRGs were immediately placed in a solution of 30% triethanolamine (TEA), 40% formamide, (F) and 30% nanopore water ($H_20$), for 15 minutes at room temperature on a shake plate, then transferred to a solution of 60% TEA, 25% F, and 15% $H_20$ for 15 minutes at room temperature on a shake plate, and finally transferred to a final solution of 70% TEA, 15% F, and 15% $H_20$ for 15-20 minutes (until clear). DRGs were then transferred into imaging chambers mounted on glass microscope slides. Imaging chambers were designed in house to be 400 µm high and fit 22 x 30 mm coverslips with a leakproof seal. Chambers were 3D printed using 3D resyn CR UHT, ApplyLabWork Tan, or polypropylene. Native mCherry expressing DRGs were then imaged on an inverted Leica TCS SP5 Confocal microscope at 10x to view the entire DRG or 63x for high resolution images. Images were analyzed using Imaris (bitplane) and ImageJ. Individual mCherry positive neurons were converted into 3D meshes within Imaris and quantified for volume and raw pixel intensity values. Data was analyzed in Prism and SPSS.

*Animal Experiments*

All animal procedures were performed in accordance with protocols approved by the Institutional Animal Care and Use Committee (IACUC) of the University of California,

San Diego. All mice were acquired from Jackson Laboratory. Two-month-old adult male C57BL/6J mice (25-30g) were housed with food and water provided *ad libitum*, under a 12 h light/dark cycle with up to 5 mice per cage. All behavioral tests were performed during the light cycle period.

*Intrathecal AAV Injections*

Anesthesia was induced with 2.5% isoflurane delivered in equal parts $O_2$ and room air in a closed chamber until a loss of the righting reflex was observed. The lower back of mice was shaven and swabbed with 70% ethanol. Mice were then intrathecally (i.t.) injected using a Hamilton syringe and 30G needle as previously described *(75)* between vertebrae L4 and L5 with 5 µL of AAV for a total of $1 \times 10^{12}$ vg/mouse, unless otherwise noted in the manuscript. All CRISPR-dCas9 experiments received $1 \times 10^{12}$ vg/mouse for each split-dCas9 AAV. A tail flick was considered indicative of appropriate needle placement. Following injection, all mice resumed motor activity consistent with that observed prior to i.t. injection.

*Pain Models*

Intraplantar carrageenan injection: Carrageenan-induced inflammation is a classic model of edema formation and hyperalgesia *(76–78)*. 21 days after AAV pre-treatment, anesthesia was induced as described above. Lambda carrageenan (Sigma Aldrich; 2% (W/V) dissolved in 0.9% (W/V) NaCl solution, 20 µL) was subcutaneously injected with a 30G needle into the plantar (ventral) surface of the ipsilateral paw. An equal amount of isotonic saline was injected into the contralateral paw. Paw thickness was measured with a caliper before and 4h after carrageenan/saline injections as an index of edema/inflammation. Hargreaves testing was performed before injection (t=0) and (t= 30, 60, 120, 240 minutes and 24 hours post-injection). The experimenter was blinded to the composition of treatment groups. Mice were euthanized after the 24-hour time point.

Paclitaxel-induced neuropathy: Paclitaxel (Tocris Biosciences, 1097) was dissolved in a mixture of 1:1:18 [1 volume ethanol/1 volume Cremophor EL (Millipore, 238470)/18 volumes of sterilized 0.9% (W/V) NaCl solution]. Paclitaxel injections (8 mg/kg) were administered intraperitoneally (i.p.) in a volume of 1 mL/100 g body weight every other day for a total of four injections to induce neuropathy (32 mg/kg), resulting in a cumulative human equivalent dose of 28.4–113.5 mg/m$^2$ as previously described *(34)*. Behavioral tests were performed 24 hours or 105 days after the last dosage for mice that

were pretreated with AAV, or 23-30 days after the last paclitaxel dosage for mice in post-chronic pain models.

Intrathecal BzATP injection: BzATP (2′(3′)-O-(4-Benzoylbenzoyl) adenosine 5′-triphosphate triethylammonium salt) was purchased from Millipore Sigma and, based on previous tests, was dissolved in saline (NaCl 0.9%) to final a concentration of 30 nmol. Saline solution was also used as a vehicle control and both were delivered in a 5 µL volume. Intrathecal injections were performed under isoflurane anesthesia (2.5%) by lumbar puncture with a 30-gauge needle attached to a Hamilton syringe.

*Pain behavioral tests*

Mice were habituated to the behavior and to the experimental chambers for at least 30 min before testing. As a positive comparator, gabapentin (Sigma, G154) was dissolved in saline solution and injected i.p. at 100 mg/kg one hour before behavioral testing.

Thermal Withdrawal Latency (Hargreaves Test): To determine the acute nociceptive thermal threshold, the Hargreaves' test was conducted using a plantar test device (Ugo Basile, Italy) *(79)*. Animals were allowed to freely move within a transparent plastic enclosure (6 cm diameter × 16 cm height) on a glass floor 40 min before the test. A mobile radiant heat source was then placed under the glass floor and focused onto the hind paw. Paw withdrawal latencies were measured with a cutoff time of 30 seconds. An IR intensity of 40 was employed. The heat stimulation was repeated three times on each hind paw with a 10 min interval to obtain the mean latency of paw withdrawal. The experimenter was blinded to composition of treatment groups.

Tactile allodynia: For the BzATP pain model, tactile thresholds (allodynia) were assessed 30 minutes, 1, 2, 3, 6, 24 hours after the BzATP injection. For the paclitaxel model, tactile thresholds (allodynia) were assessed 24 hours and 105 days after the last paclitaxel injection for mice pretreated with AAV, or 21-28 days after the last paclitaxel injection for mice that were first treated with paclitaxel and then with AAV after confirming chronic pain (post-chronic pain model). Forty-five minutes before testing, mice were placed in clear plastic wire mesh-bottom cages for acclimation. The 50% probability of withdrawal threshold was assessed using von Frey filaments (Seemes

Weinstein von Frey anesthesiometer; Stoelting Co.) ranging from 2.44 to 4.31 (0.04–2.00 g) in an up-down method, as previously described *(78)*.

Cold allodynia: Cold allodynia was measured by applying drops of acetone to the plantar surface of the hind paw as previously described *(71, 80)*. Mice were placed in individual plastic cages on an elevated platform and were habituated for at least 30 min until exploratory behaviors ceased. Acetone was loaded into a one mL syringe barrel with no needle tip. One drop of acetone (approximately 20 µL) was then applied through the mesh platform onto the plantar surface of the hind paw. Care was taken to gently apply the bubble of acetone to the skin on the paw without inducing mechanical stimulation through contact of the syringe barrel with the paw. Paw withdrawal time in a 60s observation period after acetone application was recorded. Paw withdrawal behavior was associated with secondary animal responses, such as rapid flicking of the paw, chattering, biting, and/or licking of the paw. Testing order was alternated between paws (right and left) until five measurements were taken for each paw. An interstimulation interval of 5 minutes was allowed between testing of right and left paws.

*Tissue collection*

Spinal cords were removed via hydroextrusion (injection of 2 mL of iced saline though a short blunt 20 gauge needle placed into the spinal canal following decapitation). After spinal cord tissue harvest, the L4-L6 DRG on each side were combined and frozen as for the spinal cord. Samples were placed in DNase/RNase-free 1.5 mL centrifuge tubes, quickly frozen on dry ice, and then stored at 80°C for future analysis.

*Gene Expression Analysis and qPCR*

RNA from Neuro2a cells was extracted using RNeasy Kit (QIAGEN; 74104) and from DRG using RNeasy Micro Kit (QIAGEN; 74004). cDNA was synthesized from RNA using Protoscript II Reverse Transcriptase Kit (NEB; E6560L). Real-time PCR (qPCR) reactions were performed using the KAPA SYBR Fast qPCR Kit (Kapa Biosystems; KK4601), with gene-specific primers in technical triplicates and in biological triplicates (Neuro2a cells), or in technical triplicates and biological replicates (various) for all in vivo studies. Relative mRNA expression was normalized to GAPDH and fold change was calculated using the comparative CT (ΔΔCT) method and normalized to GAPDH. Mean fold change and SD were calculated using Microsoft Excel And GraphPad Prism.

*RNA-sequencing*

RNA-Seq fastq files were mapped to GRCm38 and quantified read counts were mapped to each gene's exon using Ensembl v97 and STAR aligner *(81)*. The counts were then inputted to DESeq2 *(82)* for differential expression analysis, with log fold changes computed using the apeglm shrinkage estimator. Genes with an adjusted p-value less than 0.01 were considered to be significantly differentially expressed.

*Toxicity/Side Effect Test Battery*

*Body weights.* Body weights were recorded to the nearest 0.1g using a compact portable scale (#CB; Braintree Scientific).

*Rectal body temperatures.* Core body temperatures were measured using a digital thermometer (Body Temperature Thermometer, 50316, Stoelting Co.), with a mouse rectal probe (#RET; 3/4" length, 0.028" diameter; Braintree Scientific).

*Grip strength test.* Grip strength was measured with a mouse Grip Strength Meter (Columbus Instruments) according to the manufacturer's instructions (User Manual 0167-007). All-limb measurements were performed with the angled grid attachment, pulling the mouse towards the meter by the tail after engagement of all limbs. 5 consecutive measurements per mouse are taken and the highest 3 values are averaged, and data are expressed as newtons of peak force divided by the mouse's weight.

*Rotarod test.* A Rota-rod Series 8 apparatus (IITC Life Sciences) was used which records test results when the animal drops onto the individual sensing platforms below the rotating rod. Mice were subjected to an accelerating test strategy whereby the rod starts at 0 rpm and then accelerates at 10 rpm*(83, 84)*. The mice were tested in 3 set of 3 trials.

*Marble burying.* The marble burying test was used to assess anxiety-like *(85)* and possibly obsessive-compulsive-like behavior *(86)* capitalizing on a species-typical behavior of digging *(41)*. Importantly, this test appears to be able to capture the

anxiogenic-like behavior associated with painful states *(87, 88)*. Mice were placed individually in standard mouse cages containing bedding that is 5 cm in depth, with 20 small marbles arranged in 4 evenly spaced rows of 5 on top of the bedding material. After 30 min mice were removed and the number of marbles buried (at least 2/3 covered by bedding) is determined.

*Nest building*. Nest building is a natural rodent behavior that relates to reproduction, temperature regulation, shelter, and social behaviors. Approximately 1 h before the dark phase, mice were transferred to individual testing cages with wood-chip bedding but no environmental enrichment items such as paper towel. Nestlet material (3 g) was then placed in each cage. The nests were assessed at 2, 4, 6, 8, and 12 hr on a rating scale of 1–5 based on nest construction *(41)*. Mice were then returned to their original cages.

*Olfactory test*. This test examines the ability of a mouse to locate a desired food item buried under bedding. Mice were food restricted for 4 days (day 1- no food, day 2- 1.5 g food, day 3 & 4 – 1 g food + 1 piece chocolate puff cereal). Mice were monitored carefully, and body weights are recorded daily. On day 4 each mouse was placed in a clean cage with 2 inches bedding to habituate for 20 min. The mouse was removed, and a chocolate puff cereal was placed on top of the bedding. The mouse was then put back in the opposite end of the cage and the latencies to approach the pellet and manipulate the cereal were recorded. This test is primarily used to confirm that the mouse is motivated to find and eat the cereal. On day 5, the exact same procedure was used, but now the cereal piece is completely covered with bedding material. Again, latencies to locate and handle the cereal were recorded.

*Cognitive test – Novel object recognition test*. This test assays recognition memory while leaving the spatial location of the objects intact and is believed to involve the hippocampus, perirhinal cortex, and raphe nuclei *(89–91)*. The basic principle is that animals explore novel environments and that with repeated exposure decreased exploration ensues (habituation) *(92)*. A subsequent object substitution (replacing a familiar object with a novel object) results in dishabituation of the previously habituated exploratory behavior *(92, 93)*. The resulting dishabituation is expressed as a preferential exploration of the novel object relative to familiar features in the environment. This dishabituation has generally been interpreted as an expression of the animal's

recognition memory: the novel object is explored preferentially because it differs from what the animal remembers*(94)*. Mice were individually habituated to a 51cm x 51cm x 39cm open field for 5 min. Mice were then tested with two identical objects placed in the field (either two 250 ml amber bottles or two clear plastic cylinders 6x6x16cm half filled with glass marbles). An individual animal was allowed to explore for 5 min, now with the objects present. After two such trials (each separated by 1 minute in a holding cage), the mouse was tested in the object novelty recognition test in which a novel object replaces one of the familiar objects (for example, an amber bottle if the cylinders were initially used). All objects and the arena are thoroughly cleaned with 70% ethanol between trials to remove odors. Behavior is video recorded and then scored for contacts (touching with nose or nose pointing at object and within 0.5 cm of object). Habituation to the objects across the familiarization trials (decreased contacts) is an initial measure of learning and then renewed interest (increased contacts) in the new object indicates successful object memory.

*H&E Staining*

Two-month-old C57BL/6J male mice were injected i.t. with $1\times10^{10}$, $1\times10^{11}$, or $1\times10^{12}$ vg/mouse of AAV9 mCherry or AAV9 Zinc-Finger-4. 21 Days following i.t. injections, mice were transcardially perfused with 4% PFA and lumbar DRG were post-fixed in 4% PFA for 24 hours, stored in PBS with 0.02% sodium azide, and sectioned using standard protocols.

*Histopathology analysis*

H&E stained paraffin sections (blinded to experimental condition), were reviewed independently by three neuropathologists. After independent review, the findings were reviewed in a group for discussion and to find points of consensus.

*Multielectrode array recording*

Action potential firing was measured using a multiwell MEA system (Maestro, Axion Biosystems). In each experiment, DRG neurons from male C57BL/6J were seeded in a 6-well MEA recording plate (2 wells for each animal). AAV was then added to each well at $1\times10^{11}$ vg/well, and after sufficient recovery time, measurements were taken. The investigator was blinded to the identity of the virus added. To collect measurements, MEA plates were placed in the reader with the reader plate heater set to either 37℃ and

42 ℃ and under 95% $O_2$/5% $CO_2$ air flow. Plates were allowed to equilibrate to these conditions for a minimum of 5 minutes before collecting spontaneous recordings for 180 seconds. Electrical signals were collected and analyzed using the AxIS Software and Neural Metric Tool (Axion Biosystems) with Spontaneous Neural configuration. Signals were filtered with a band-pass filter of 200 Hz – 3 kHz. Spikes were detected with AxIS software using an adaptive threshold crossing set to 5.5 times the standard deviation of the estimated noise for each electrode.

*RNAscope ISH Assays*

The $Na_V1.7$ probe was designed by Advanced Cell Diagnostics (ACD Cat#313341) and was designed to detect detect 3404–4576 bp of the *Mus musculus* $Na_V1.7$ mRNA sequence (NM_018852.2, C3 channel). DRG were placed into paraffin, sectioned (12 $\mu$m thick), and mounted on positively charged microscopic glass slides (Fisher Scientific). All hybridization and amplification steps were performed following the ACD RNAscope V2 Formalin-Fixed Paraffin-Embedded (FFPE) sample preparation protocol. Cover slips were added on stained slides with fluorescent mounting medium (ProLong Gold Anti-fade Reagent P36930; Life Technologies) and scanned into digital images with a Zeiss 880 Airyscan Confocal at 20x magnification. Data was processed using ZEN software (manufacturer-provided software).

*Quantification of RNAscope Signal.* Full-size confocal images were converted to 8-bit greyscale in ImageJ. A universal threshold was applied across all images, and particles were counted. All particles with an area below 30 pixels were treated as representing a single probe. For particles of larger pixel area, the total pixel area was divided by 30 to obtain the approximate number of probes represented by a given particle. Individual DRG cells were identified via DAPI stains and counted manually to obtain the total number of DRG cells on each image. The average number of probes per cell was then obtained by dividing the total number of probes by the total number of DRG cells.

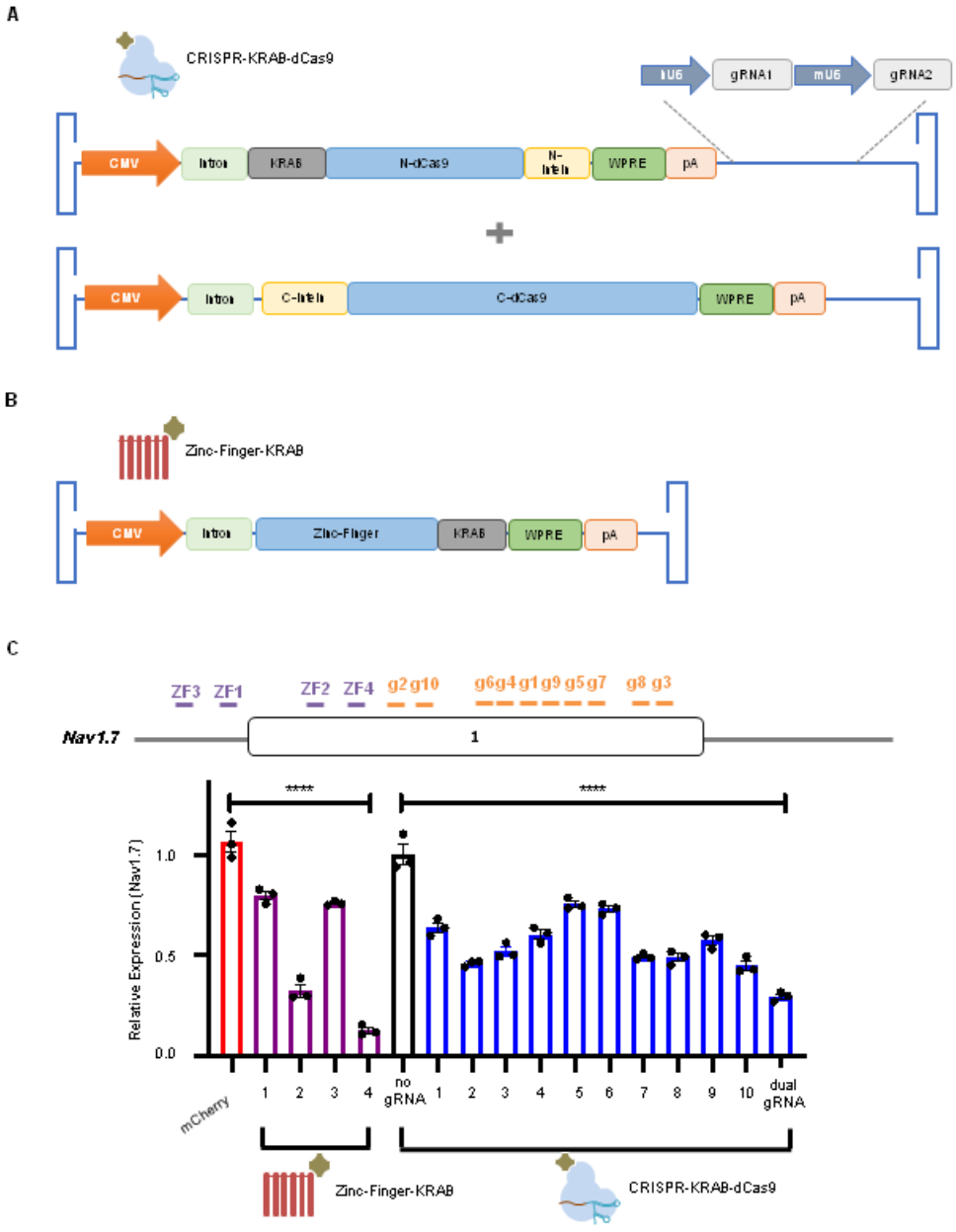


**Fig. S1. In vitro optimization of epigenetic genome engineering tools to enable $Na_V1.7$ repression. (A)** Schematic of a dual-pAAV intein-mediated split-*Streptococcus pyogenes* dead Cas9 (dCas9) for genome regulation. **(B)** Schematic of Zinc-Finger

pAAV for genome regulation. **(C)** A panel of four zinc finger proteins and ten gRNAs were designed to target $Na_V1.7$ in a mouse neuroblastoma cell line (Neuro2a) and were screened for repression efficacy by qPCR. A non-targeting gRNA (no gRNA) was used as a control for -dCas9 constructs targeting $Na_V1.7$, while mCherry was used as a control for ZFP-KRAB constructs targeting $Na_V1.7$ (dots represent individual biological replicates; qPCR was performed in technical triplicates; n=3; error bars are SEM; values normalized to Gapdh; one-way ANOVA with Dunnett's *post hoc* test; ****$p < 0.0001$).

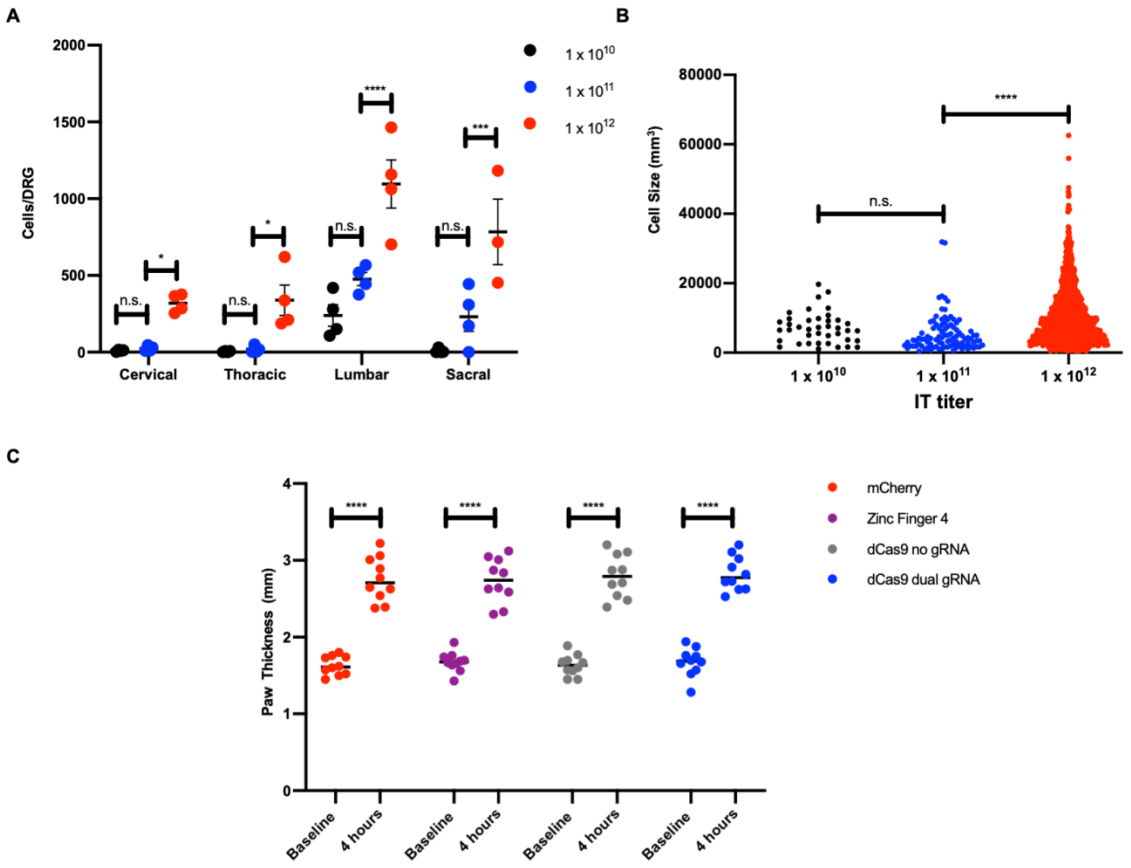


**Fig. S2. Quantification of DRG transduction efficiencies via AAVs and carrageenan-induced inflammation in mice. (A)** The number of mCherry positive cells in whole mount DRG (from Figure 2) along the neuroaxis following intrathecal injections

of AAV9-mCherry illustrating transduction efficacy at different viral titers ($1\times10^{10}$, $1\times10^{11}$, or $1\times10^{12}$ vg/mouse; dots represent individual biological replicates; n=3-4; error bars are SEM; Two-way ANOVA with Bonferroni's *post hoc* test; n.s. = not significant, *p = 0.0384, *p = 0.0224, ****p < 0.0001; ***p = 0.0002). **(B)** The cell size distribution of mCherry positive cells in mice cervical DRG following intrathecal injections of AAV9-mCherry at different viral titers ($1\times10^{10}$, $1\times10^{11}$, or $1\times10^{12}$ vg/mouse) is quantified (dots represent individual cells; One-way ANOVA with Tukey's *post hoc* test; n.s. = not significant, ****p < 0.0001). **(C)** Paw thickness of ipsilateral paws at baseline and four hours after carrageenan injection are plotted (dots represent individual biological replicates; n=10; error bars are SEM; Student's t-test; ****p < 0.0001).

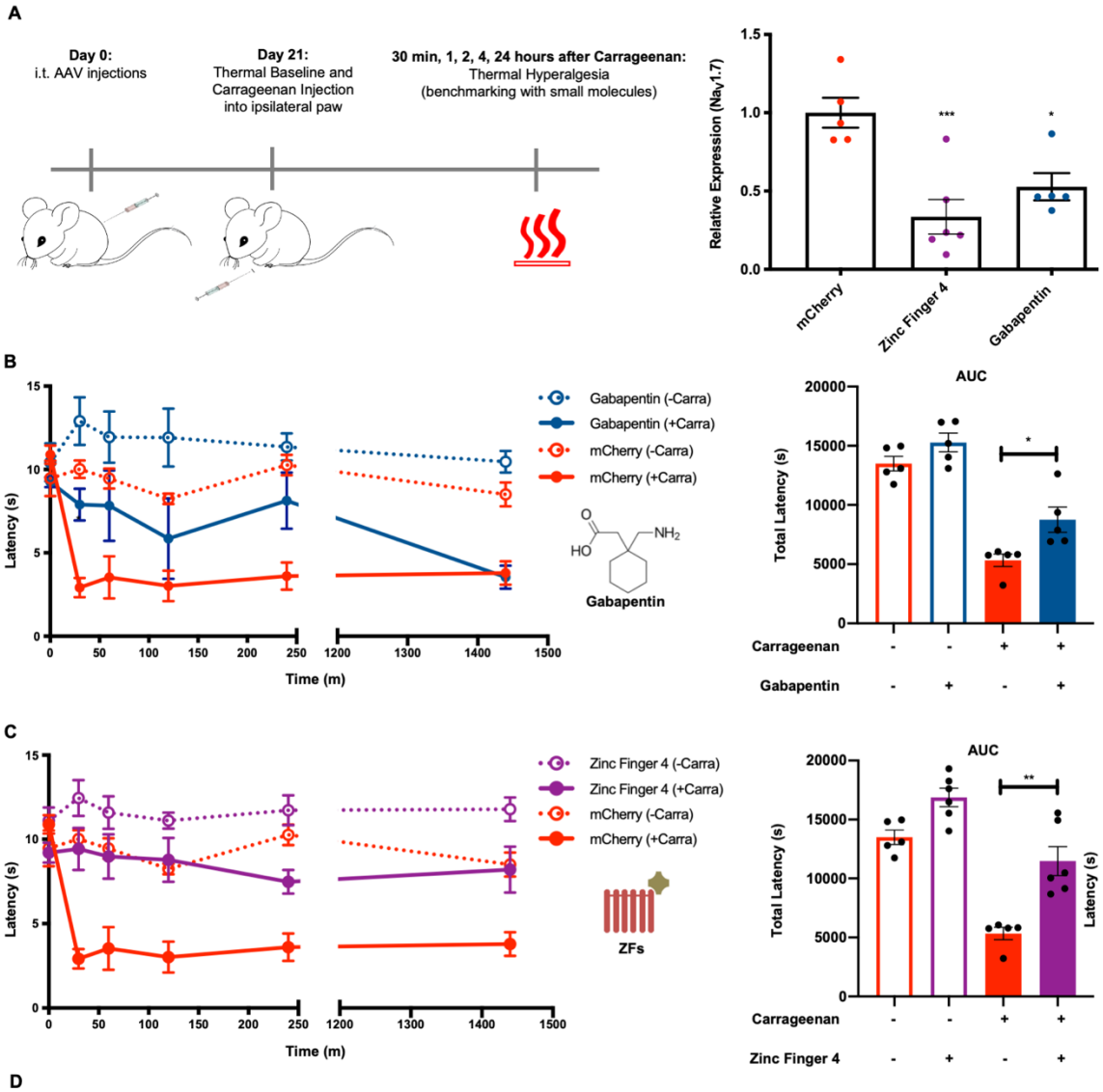


D

| Comparison | Group | Pre-carrageenan | Post-carrageenan | | | | |
|---|---|---|---|---|---|---|---|
| | | 0 minutes | 30 minutes | 1 hour | 2 hours | 4 hours | 24 hours |
| mCherry (+Carra) | ZF-4-KRAB (+Carra) | n.s. | ****p<0.0001 | ***p=0.0002 | ****p< 0.0001 | *p=0.0104 | **p=0.0028 |
| | Gabapentin (+Carra) | n.s. | **p=0.0081 | *p=0.0276 | n.s. | *p=0.0184 | n.s. |
| mCherry (-Carra) | ZF-4-KRAB (-Carra) | n.s. | n.s. | n.s. | n.s. | n.s. | n.s. |
| | Gabapentin (-Carra) | n.s. | n.s. | n.s. | n.s. | n.s. | n.s. |

**Fig. S3. Benchmarking of in situ repression of $Na_V1.7$ using ZFP-KRAB with established small-molecule drug gabapentin. (A)** In vivo $Na_V1.7$ repression efficiencies from treated mice DRG. Twenty-four hours after carrageenan administration, mice DRG (L4-L6) were harvested and $Na_V1.7$ repression efficacy was determined by qPCR (dots represent individual biological replicates; n=5 for mCherry and gabapentin

groups, n=6 for Zinc-Finger-4-KRAB group; error bars are SEM; one-way ANOVA with Dunnett's *post hoc* test; ***p = 0.0007, *p = 0.0121). **(B,C)** Time course of thermal hyperalgesia after the injection of carrageenan (solid lines) or saline (dotted lines) into the hind paw of mice injected with gabapentin (100mg/kg), AAV9-mCherry and AAV9-Zinc-Finger-4-KRAB are plotted. Mean paw withdrawal latencies (PWL) are shown. The Area Under the Curve (AUC) of the thermal-hyperalgesia time-course are plotted on the right panels. A significant increase in PWL is seen in the carrageenan-injected paws of mice injected with gabapentin and Zinc-Finger-4-KRAB (dots represent individual biological replicates; n=5 for mCherry and gabapentin, n=6 for Zinc-Finger-4-KRAB; error bars are SEM; Student's t-test, *p = 0.0208, **p = 0.0021). **(D)** Significance of paw withdrawal latencies in mice receiving AAV9-Zinc-Finger-4-KRAB and gabapentin (100 mg/kg) as compared to AAV9-mCherry carrageenan-injected paw (negative control). Two-way ANOVA with Bonferroni *post hoc* test.

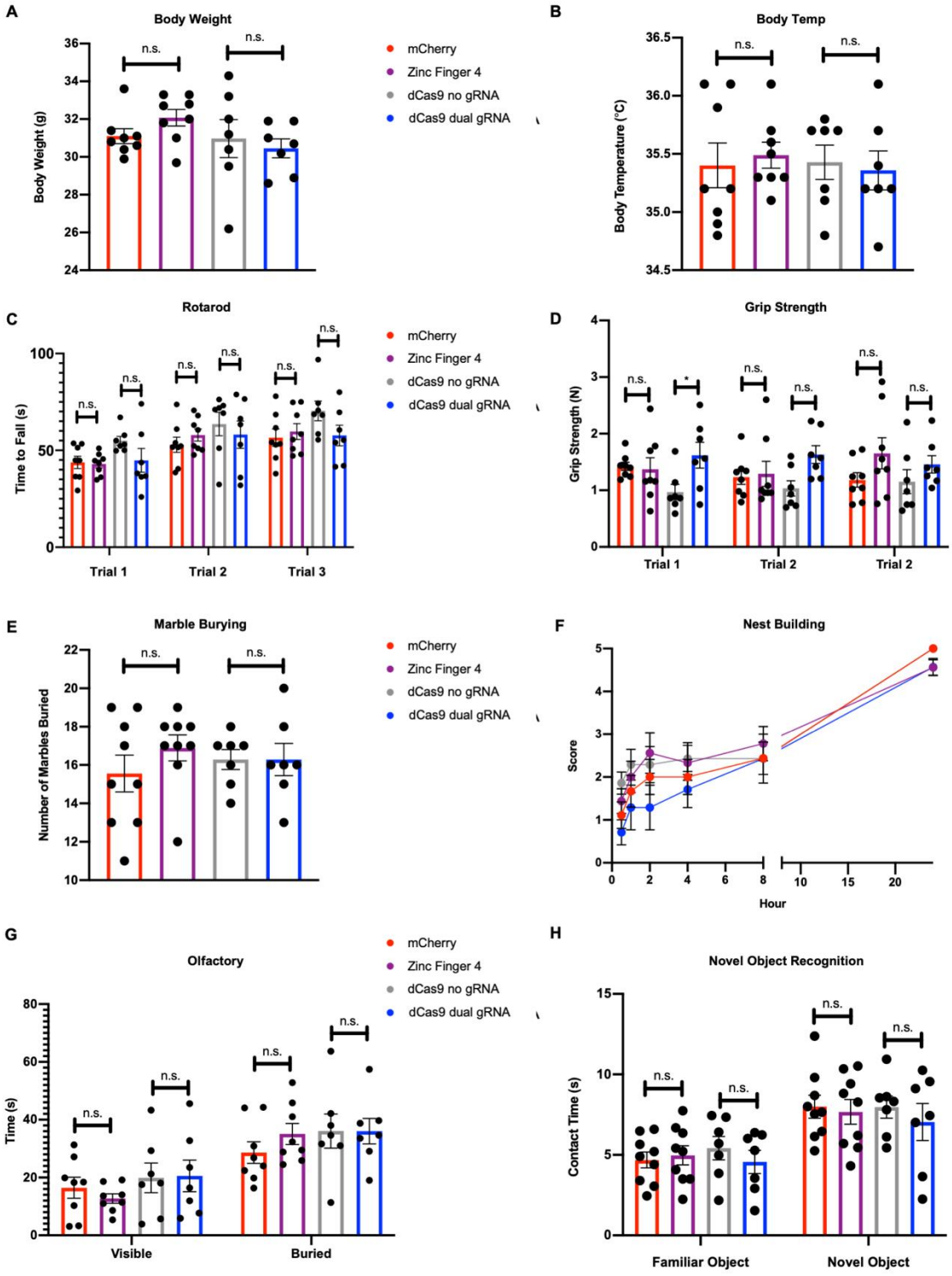


**Fig. S4. Examining the safety of in situ repression of $Na_V1.7$ via ZFP-KRAB and KRAB-dCas9. (A)** Body weight of mice injected with AAV9-mCherry, AAV9-Zinc-Finger-4-KRAB, AAV9-KRAB-dCas9-no-gRNA, and AAV9-KRAB-dCas9-dual-gRNA are plotted (dots represent individual biological replicates; n=8 for mCherry and Zinc-Finger-4

groups and n=7 for dCas9-no-gRNA and dCas9-dual-gRNA groups; error bars are SEM; Student's t-test; n.s. = not significant). **(B)** Body temperature of mice injected with AAV9-mCherry, AAV9-Zinc-Finger-4-KRAB, AAV9-KRAB-dCas9-no-gRNA, and AAV9-KRAB-dCas9-dual-gRNA are plotted (dots represent individual biological replicates; n=8 for mCherry and Zinc-Finger-4 groups and n=7 for dCas9-no-gRNA and dCas9-dual-gRNA groups; error bars are SEM; Student's t-test; n.s. = not significant). **(C)** Rotarod studies to determine motor coordination and balance of mice injected with AAV9-Zinc-Finger-4-KRAB and AAV9-KRAB-dCas9-dual-gRNA (dots represent individual biological replicates; n=8 for mCherry and Zinc-Finger-4 groups and n=7 for dCas9-no-gRNA and dCas9-dual-gRNA groups; error bars are SEM; Two-way ANOVA with Bonferroni *post hoc* test; n.s. = not significant). **(D)** No significant changes in grip strength was seen in mice injected with AAV9-mCherry, AAV9-Zinc-Finger-4, AAV9-KRAB-dCas9-no-gRNA, and AAV9-KRAB-dCas9-dual-gRNA (dots represent individual biological replicates; n=8 for mCherry and Zinc-Finger-4 groups and n=7 for dCas9-no-gRNA and dCas9-dual-gRNA groups; error bars are SEM; Two-way ANOVA with Bonferroni *post hoc* test; *p = 0.0402, n.s. = not significant). **(E)** The number of marbles buried by mice injected with AAV9-mCherry, AAV9-Zinc-Finger-4, AAV9-KRAB-dCas9-no-gRNA, and AAV9-KRAB-dCas9-dual-gRNA are plotted (dots represent individual biological replicates; n=8 for mCherry and Zinc-Finger-4 groups and n=7 for dCas9-no-gRNA and dCas9-dual-gRNA groups; error bars are SEM; Student's t-test; n.s. = not significant). **(F)** Nest building scores demonstrated no significant changes between experimental and control groups (dots represent individual biological replicates; n=8 for mCherry and Zinc-Finger-4 groups and n=7 for dCas9-no-gRNA and dCas9-dual-gRNA groups; error bars are SEM; Two-way ANOVA with Bonferroni *post hoc* test). **(G)** An olfactory test was performed to determine whether knockdown of $Na_V1.7$ via AAV9-Zinc-Finger-4-KRAB and AAV9-KRAB-dCas9-dual-gRNA causes anosmia. No significant olfactory detection changes were seen in mice injected with AAV9-Zinc-Finger-4-KRAB and AAV9-KRAB-dCas9-dual-gRNA as compared to the control groups, AAV9-mCherry and AAV9-KRAB-dCas9-no gRNA, respectively (dots represent individual biological replicates; n=8 for mCherry and Zinc-Finger-4 groups and n=7 for dCas9-no-gRNA and dCas9-dual-gRNA groups; error bars are SEM; One-way ANOVA with Bonferroni *post hoc* test; n.s. = not significant). **(H)** A novel object recognition test showed comparable memory retention in mice injected with AAV9-Zinc-Finger-4-KRAB and AAV9-KRAB-dCas9-dual-gRNA as compared to the control groups, AAV9-mCherry and AAV9-KRAB-dCas9-no gRNA,

respectively (dots represent individual biological replicates; n=8 for mCherry and Zinc-Finger-4 groups and n=7 for dCas9-no-gRNA and dCas9-dual-gRNA groups; error bars are SEM; One-way ANOVA with Bonferroni *post hoc* test; n.s. = not significant).

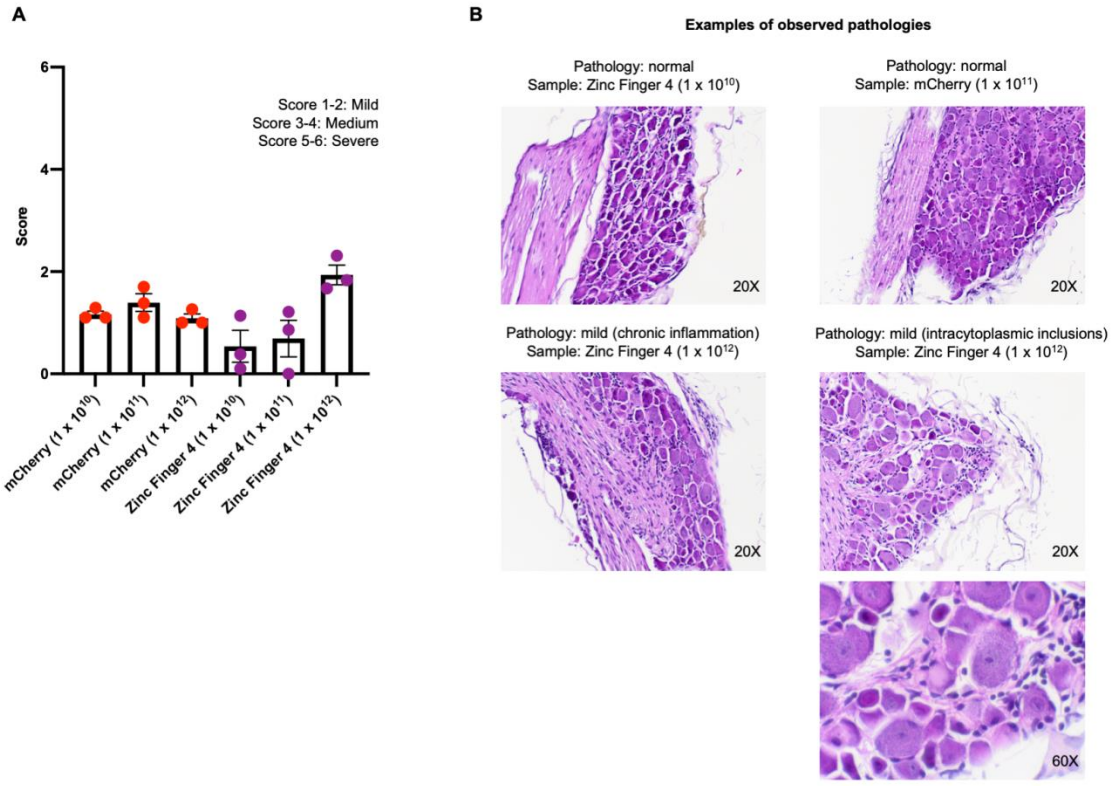


**Fig. S5. Neuropathology analyses of DRGs targeted via AAVs. (A)** H&E stained paraffin sections (blinded to experimental condition), were reviewed independently by three neuropathologists. After independent review, the findings were reviewed in a group

for discussion and to find points of consensus. In all cases, the DRGs showed no loss of neurons, and the nerves showed no axonal injury or myelin pathology (dots represent individual biological replicates; n=3; error bars are SEM). **(B)** In one case, DRG neurons showed intracytoplasmic inclusions of unknown significance (image depicted in panel b). In another case, focal mild chronic inflammation was seen (image depicted in panel b). These two cases also scored highest on semiquantitative pathology scoring. Other cases appeared normal (representative images depicted in panel b) or showed only mild or questionable findings (such as questionable mild nerve edema).

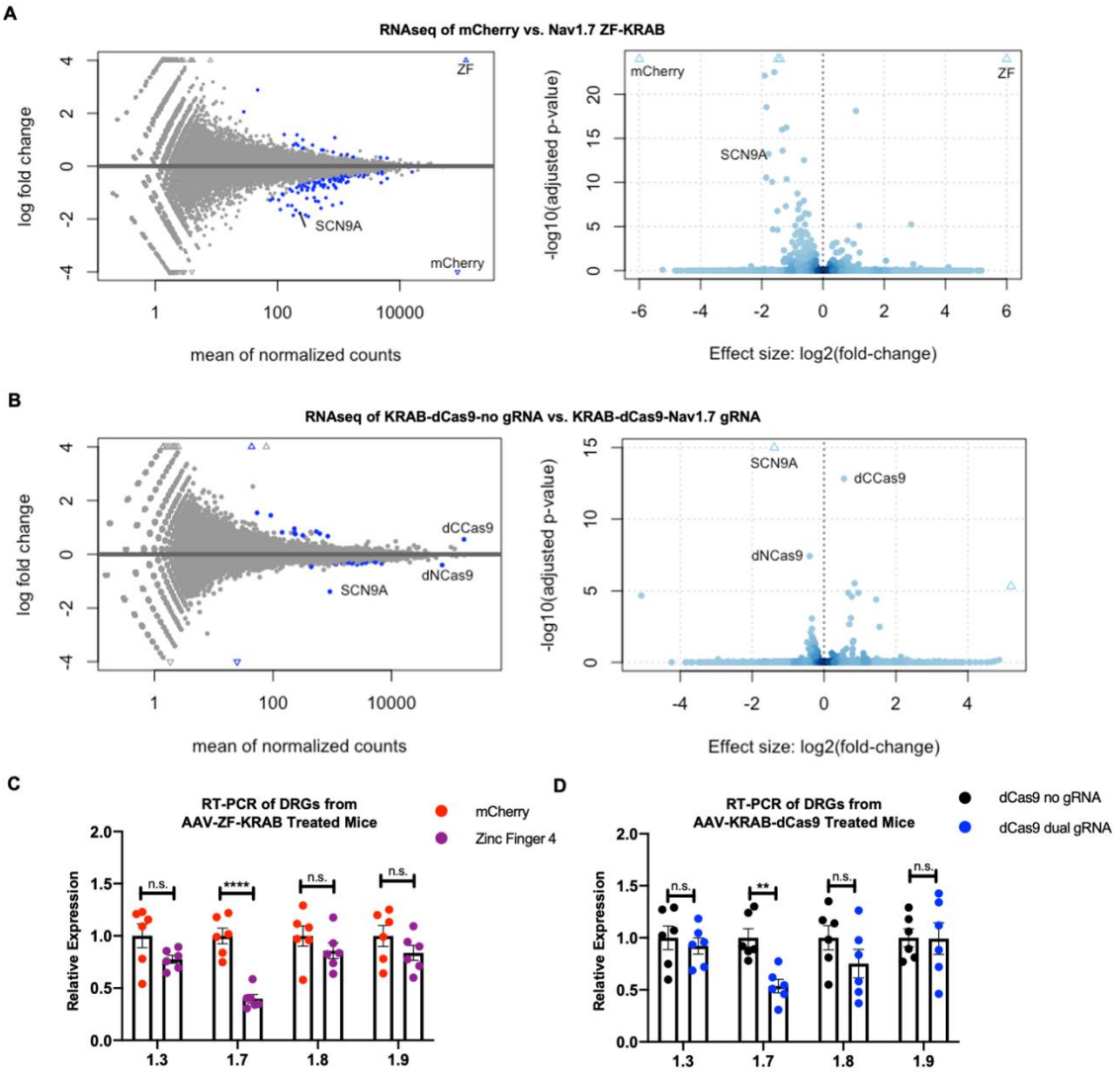


**Fig. S6. Genome-wide analysis of gene expression in zinc finger or CRISPR-treated Neuro2a cells. (A)** Blue data points indicate FDR < 0.01 by differential-expression analysis (n = 3 for Neuro2a). The data points representing the ZF and mCherry transcripts are highlighted as blue triangles. **(B)** Blue data points indicate FDR < 0.01 by differential-expression analysis (n = 3 for Neuro2a). The data points representing the dNCas9 and dCCas9 are highlighted as blue triangles **(C)** Following paclitaxel administration and i.t. AAV9 delivery (Fig. 4), mice DRG (L4-L6) were harvested and $Na_V1.3$, $Na_V1.7$**,** $Na_V1.8$, and $Na_V1.9$ expression relative to Gapdh were determined by qPCR in mice injected with AAV9-mCherry or AAV9-Zinc-Finger-4-KRAB (dots represent individual biological replicates; n=6; error bars are SEM; Student's t-test; ****p < 0.0001, n.s. = not significant). **(D)** Following paclitaxel administration and i.t. AAV9 delivery (Fig. 4), mice DRG (L4-L6) were harvested and $Na_V1.3$, $Na_V1.7$ **,** $Na_V1.8$,

and $Na_V1.9$ expression relative to Gapdh were determined by qPCR in mice injected with AAV9-KRAB-dCas9-no-gRNA or AAV9-KRAB-dCas9-dual-gRNA (dots represent individual biological replicates; n=6; error bars are SEM; Student's t-test; **p = 0.0092, n.s. = not significant).

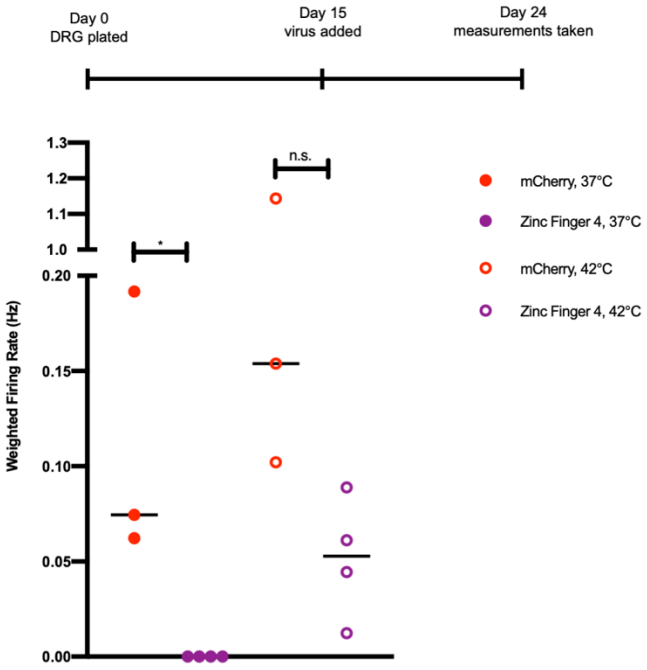


**Fig. S7. Multielectrode array recordings of DRG neurons transduced with AAV9-Zinc-Finger-4 show reduced response to heat.** Weighted firing rate from DRG transduced with AAV9-mCherry or AAV9-Zinc-Finger-4-KRAB is graphed (dots represent individual biological replicates; n=3 AAV9 mCherry and n=4 for AAV9 Zinc-Finger-4-KRAB transduced wells; Student's t-test; *p = 0.0248; n.s. = not significant).

**Table S1. CRISPR-Cas9 gRNA spacer sequences.**

| gRNA | Sequence |
|---|---|
| SCN9A-1 | ACAGTGGGCAGGATTGAAA |
| ~~SCN9A-3~~ | ~~GCAGGTGCACTCACCGGGT~~ |
| ~~SCN9A-2~~ | ~~GAGCTCAGGGAGCATCGAGG~~ |
| SCN9A-4 | AGAGTCGCAATTGGAGCGC |
| SCN9A-5 | CCAGACCAGCCTGCACAGT |
| SCN9A-6 | GAGCGCAGGCTAGGCCTGCA |
| SCN9A-7 | CTAGGAGTCCGGGATACCC |
| SCN9A-8 | GAATCCGCAGGTGCACTCAC |
| SCN9A-9 | GACCAGCCTGCACAGTGGGC |
| SCN9A-10 | GCGACGCGGTTGGCAGCCGA |

**Table S2. ZFP genomic target sequences.**

| ZF Name | ZF Target Sequence | ZF Protein Sequence |
|---|---|---|
| ZF1 | GGCGAGGTGATGGAAGGG | RSMHDYKDHDGDYKDHDIDY<br>KDDDDKMAPKKKRKVGIHGV<br>PAAMAERPFQCRICMRNFSR<br>SAHLSRHIRTHTGEKPFACD<br>ICGRKFAQSGNLARHTKIHT<br>GSQKPFQCRICMRNFSRSDA<br>MSQHIRTHTGEKPFACDICG<br>RKFARNASRTRHTKIHTGSQ<br>KPFQCRICMRNFSRSANLAR<br>HIRTHTGEKPFACDICGRKF<br>ADRSHLARHTKIHLRQKDAA<br>RGSRTLVTFKDVFVDFTREE<br>WKLLDTAQQIVYRNVMLENY<br>KNLVSLGYQLTKPDVILRLE<br>KGEEPWLVDYKDDDDKRS |
| ZF2 | GAGGGAGCTAGGGGTGGG | RSMHDYKDHDGDYKDHDIDY<br>KDDDDKMAPKKKRKVGIHGV<br>PAAMAERPFQCRICMRNFSR<br>SANLARHIRTHTGEKPFACD<br>ICGRKFADSSDRKKHTKIHT<br>GSQKPFQCRICMRNFSTSGS<br>LSRHIRTHTGEKPFACDICG<br>RKFAHSLSLKNHTKIHTGSQ<br>KPFQCRICMRNFSQSSDLSR<br>HIRTHTGEKPFACDICGRKF<br>AWKWNLRAHTKIHLRQKDAA<br>RGSRTLVTFKDVFVDFTREE<br>WKLLDTAQQIVYRNVMLENY<br>KNLVSLGYQLTKPDVILRLE<br>KGEEPWLVDYKDDDDKRS |
| ZF3 | AGTGCTAATGTTTCCGAG | RSMHDYKDHDGDYKDHDIDY<br>KDDDDKMAPKKKRKVGIHGV<br>PAAMAERPFQCRICMRNFSR<br>SAHLSRHIRTHTGEKPFACD<br>ICGRKFATSGHLSRHTKIHT<br>GSQKPFQCRICMRNFSRSDH<br>LSQHIRTHTGEKPFACDICG<br>RKFAASSTRTKHTKIHTGSQ<br>KPFQCRICMRNFSQSSHLTR<br>HIRTHTGEKPFACDICGRKF<br>ARSDNLTRHTKIHLRQKDAA<br>RGSRTLVTFKDVFVDFTREE<br>WKLLDTAQQIVYRNVMLENY |

| | | |
|---|---|---|
| | | KNLVSLGYQLTKPDVILRLE<br>KGEEPWLVDYKDDDDKRS |
| ZF4 | TAGACGGTGCAGGGCGGA | RSMHDYKDHDGDYKDHDIDY<br>KDDDDKMAPKKKRKVGIHGV<br>PAAMAERPFQCRICMRNFSD<br>RSHLTRHIRTHTGEKPFACD<br>ICGRKFADRSHLARHTKIHT<br>GSQKPFQCRICMRNFSRSDN<br>LSEHIRTHTGEKPFACDICG<br>RKFARSAALARHTKIHTGSQ<br>KPFQCRICMRNFSRSDTLSQ<br>HIRTHTGEKPFACDICGRKF<br>ATRDHRIKHTKIHLRQKDAA<br>RGSRTLVTFKDVFVDFTREE<br>WKLLDTAQQIVYRNVMLENY<br>KNLVSLGYQLTKPDVILRLE<br>KGEEPWLVDYKDDDDKRS |

**Table S3. qPCR primers.**

| Gene | Forward | Reverse |
|---|---|---|
| Gapdh | TGGCCTTCCGTGTTCCTAC | GAGTTGCTGTTGAAGTCGCA |
| Scn3a | GGGCCTTCTTATCGCTGTTTCG | CCCAGCTGCACGTAATGTCAAC |
| Scn9a | GGCAGAAGCTGAGCCTATCAATGC | TGGAAATCTCCTCACACAGCCATC |
| Scn10a | TTTCCGAGCACAGAGGGCAATG | CAGCTTAGACTCTTCCAGCTCCTC |
| Scn11a | TTCTTGGCTTCCCTCAGAGTGC | GTGTTTAATGTGGGCCAGGATTTG |